THE JOURNAL OF BIOLOGICAL CHEMISTRY VOL. 282, NO. 49, pp. 35787–35795, December 7, 2007

Structural Basis of Ubiquitin Recognition by the Ubiquitin-associated (UBA) Domain of the Ubiquitin Ligase EDD*[S]

Received for publication, July 10, 2007, and in revised form, August 29, 2007 Published, JBC Papers in Press, September 25, 2007, DOI 10.1074/jbc.M705655200

Guennadi Kozlov[‡], Long Nguyen[‡], Tong Lin[§¶], Gregory De Crescenzo[‖1], Morag Park[‡§¶2], and Kalle Gehring[‡3]**

*From the [‡]Department of Biochemistry, McGill University, Montréal, Québec H3G 1Y6, Departments of [§]Medicine, and **Oncology, McGill University and [¶]Molecular Oncology Group, McGill University Health Centre, Montréal, Québec H3A 1A1, and the [‖]Département de Génie Chimique, École Polytechnique de Montréal, Montréal, Québec H3T 1J4, Canada*

EDD (or HYD) is an E3 ubiquitin ligase in the family of HECT (homologous to E6-AP C terminus) ligases. EDD contains an N-terminal ubiquitin-associated (UBA) domain, which is present in a variety of proteins involved in ubiquitin-mediated processes. Here, we use isothermal titration calorimetry (ITC), NMR titrations, and pull-down assays to show that the EDD UBA domain binds ubiquitin. The 1.85 Å crystal structure of the complex with ubiquitin reveals the structural basis of ubiquitin recognition by UBA helices α1 and α3. The structure shows a larger number of intermolecular hydrogen bonds than observed in previous UBA/ubiquitin complexes. Two of these involve ordered water molecules. The functional importance of residues at the UBA/ubiquitin interface was confirmed using site-directed mutagenesis. Surface plasmon resonance (SPR) measurements show that the EDD UBA domain does not have a strong preference for polyubiquitin chains over monoubiquitin. This suggests that EDD binds to monoubiquitinated proteins, which is consistent with its involvement in DNA damage repair pathways.

The E3 isolated by differential display (EDD)[4] protein is the human ortholog of the *Drosophila melanogaster* tumor suppressor hyperplastic discs protein (HYD). Both belong to the family of HECT (homologous to E6-AP C terminus) E3 ubiquitin ligases, which target specific proteins for ubiquitin-mediated proteolysis. The highly conserved ubiquitin/proteasome pathway controls the degradation of many critical regulatory proteins. Proteins are targeted by conjugation of a 76-residue ubiquitin moiety to lysine residues via an isopeptide bond. This occurs through a combined set of reactions involving activating (E1), conjugating (E2), and ligating (E3) enzymes. E3 enzymes physically interact with their substrates and are thus critical determinants of the specificity of ubiquitination. Two main groups of E3 ubiquitin ligases include RING finger (1) and HECT domain ligases (2), the latter being found in EDD.

In *Drosophila*, EDD is required for regulation of cell proliferation during development (3). It is inferred that EDD functions in signal transduction downstream of the receptors to initiate and/or maintain proliferation as well as signals to terminate proliferation (3). Cells with mutations in EDD fail to properly terminate proliferation leading to a tumorous phenotype. The mutations also result in developmental abnormalities such as adult sterility due to germ cell defects (4). EDD is frequently overexpressed in breast and ovarian cancer supporting a potential role in cancer development (5, 6). EDD is also involved in DNA damage signaling where TopB1, a target for ubiquitinylation by EDD (7), co-localizes with BRCA1 at stalled replication forks (7, 8). Recently, EDD was shown to activate the DNA damage checkpoint kinase CHK2 (9). EDD also interacts with the calcium and integrin-binding protein (CIB) in a DNA damage-dependent manner (10). Finally, EDD is an *in vivo* substrate for the extracellular signal-regulated kinases (ERK) 1 and 2 (11). As a ubiquitin ligase, EDD was shown to control the levels of poly(A)-binding protein interacting protein 2 (Paip2) (12).

Structurally, EDD contains a ubiquitin-associated (UBA) domain at its N terminus (10), two nuclear localization signals, a zinc finger-like UBR domain involved in recognition of type 1 N-degrons (13), a domain homologous to the C-terminal domain of poly(A)-binding protein (PABC), and a HECT domain at its far C terminus. UBA domains were originally identified in a variety of proteins involved in ubiquitin-mediated processes (14, 15). The three-dimensional structure of a UBA domain shows a bundle of three α-helices (16). UBA domains generally contain surface patches of hydrophobic residues, which are involved in protein-protein interactions. Most UBA domains bind ubiquitin and ubiquitin-like (UBL) domains (17). Two structures of a UBA domain in complex with monoubiquitin determined by NMR spectroscopy show that the first

* This work was supported by CIHR Operating Grants MOP-11545 (to M. P.) and MOP-14219 (to K. G.). The costs of publication of this article were defrayed in part by the payment of page charges. This article must therefore be hereby marked "*advertisement*" in accordance with 18 U.S.C. Section 1734 solely to indicate this fact.

The atomic coordinates and structure factors (code 2QHO) have been deposited in the Protein Data Bank, Research Collaboratory for Structural Bioinformatics, Rutgers University, New Brunswick, NJ (http://www.rcsb.org/).

[S] The on-line version of this article (available at http://www.jbc.org) contains supplemental Figs. S1–S3.

[1] Holds a Canada Research Chair in Protein-enhanced Biomaterials.

[2] A senior scholar of the Canadian Institutes of Health Research (CIHR).

[3] A Chercheur National of the Fonds de la recherche en santé Québec (FRSQ). To whom correspondence should be addressed: Dept. of Biochemistry, McGill University, 3655 Promenade Sir William Osler, Montreal, Quebec H3G 1Y6, Canada. Tel.: 514-398-7287; Fax: 514-847-0220; E-mail: kalle.gehring@mcgill.ca.

[4] The abbreviations used are: EDD, E3 isolated by differential display; HYD, hyperplastic discs; HECT, homologous to E6-AP C terminus; UBA, ubiquitin-associated; CUE, coupling of ubiquitin conjugation to endoplasmic reticulum degradation; HSQC, heteronuclear single-quantum correlation spectroscopy; NOE, nuclear overhauser effect; r.m.s.d., root-mean square deviation; UBL, ubiquitin-like domain; SPR, surface plasmon resonance; ITC, isothermal titration calorimetry; GST, glutathione *S*-transferase; PDB, Protein Data Bank.

loop and the C-terminal part of helix α3 of the UBA domain bind to the β-sheet of ubiquitin centered on Ile44 (18, 19). In particular, the methionine residue from the α1–α2 loop, conserved in many UBA domains, makes key hydrophobic contacts with ubiquitin. Despite the existing structural information, the mechanism of ubiquitin recognition is still not understood for a number of UBA domains. For instance, some UBA domains do not contain the critical methionine or even a hydrophobic residue in the corresponding position and still bind to ubiquitin efficiently (20). The low sequence homology between UBA domains makes predicting and understanding their function difficult. For example, recent high-resolution crystal structures of UBA domains from Cbl ubiquitin ligases revealed that, unlike previously studied UBA domains, the Cbl-b UBA domain binds ubiquitin via UBA helix α1 (21) while the c-Cbl UBA domain dimerizes (22).

Here, we used pull-down assays, SPR, ITC, and NMR spectroscopy to show that UBA from EDD ligase binds to monoubiquitin and polyubiquitin chains. To understand the structural basis of this binding, we performed x-ray crystallography and mutational analysis of this UBA domain. We report the crystal structure of EDD UBA in complex with ubiquitin. The structure improves our understanding of ubiquitin recognition by UBA domains and provides a basis for further functional studies of the ubiquitin ligase EDD.

EXPERIMENTAL PROCEDURES

Protein Expression, Preparation, and Purification—The UBA domain from human EDD ligase (residues 180–230) was cloned into a pGEX-4T-1 vector (Amersham Biosciences) and expressed in *Escherichia coli* BL21 (DE3) in rich (LB) medium as a fusion with N-terminal GST tag. To aid quantification, an I180Y mutation was introduced into the constructs used for NMR and ITC. The wild-type sequence was used for crystallization, SPR, pull-down assays, and site-directed mutagenesis studies. GST fusion proteins were purified by affinity chromatography on glutathione-Sepharose resin, and the tag was removed by cleavage with thrombin, leaving a two-residue Gly-Ser N-terminal extension. The cleaved protein was additionally purified using size-exclusion chromatography (Superdex-75) and buffer exchanged using Centricon 5000 concentrators. For NMR experiments, the protein was labeled by growth in M9 minimal medium with [^{15}N]ammonium sulfate or [^{15}N]ammonium sulfate/[^{13}C]glucose as the sole sources of nitrogen and carbon. Bovine ubiquitin was purchased from Sigma-Aldrich and used without further purification. Site-directed mutagenesis was performed using QuikChange™ (Stratagene) and confirmed by DNA sequencing.

In Vitro Binding Assays—Expression of GST-UBA in *E. coli* BL21 was induced with 0.1 mM isopropyl-1-thio-β-D-galactopyranoside for 3 h. Bacteria were lysed by sonication in TNE buffer (50 mM Tris·Cl pH 8.0, 1% Nonidet P-40, 2 mM EDTA) containing 10% glycerol, 10 μg/ml aprotinin, 10 μg/ml leupeptin, and 1 mM phenylmethylsulfonyl fluoride (PMSF), and the lysates cleared by ultracentrifugation. Binding assays were carried out by incubating bacterial lysates containing 1 μg of GST-UBA with 12 μl of ubiquitin-agarose (120 μg of ubiquitin) (Boston Biochem, Inc.) for 2 h at 4 °C. The beads were washed extensively with TGH buffer (50 mM HEPES pH 7.5, 150 mM NaCl, 1.5 mM $MgCl_2$, 1 mM EGTA, 1% Triton X-100, 10% glycerol, 1 mM PMSF, 1 mM sodium vanadate, 10 μg/ml aprotinin, and 10 μg/ml leupeptin) and the bound proteins resolved by SDS-PAGE and immunodetection with anti-GST. Alternatively, 1 μg of GST-UBA fusion protein immobilized on glutathione Sepharose was incubated with 2 μg of either K48- or K63-linked ubiquitin chains (Boston Biochem, Inc.) for 1 h at 4 °C, washed extensively with TGH buffer, and the bound proteins resolved by SDS-PAGE and immunodetection. Anti-ubiquitin (P4D1) and anti-GST (B-14) antibodies were purchased from Santa Cruz Biotechnology.

Isothermal Titration Calorimetry (ITC) Measurements—Experiments were carried out on a MicroCal VP-ITC titration calorimeter (MicroCal Inc., Northampton, MA) using the VPViewer software for instrument control and data acquisition. The buffer used for ITC experiments contained 25 mM phosphate buffer (pH 7.0), 70 mM NaCl. During a titration experiment, 50 μM sample of UBA from EDD was thermostatted at 293 K in a stirred (260 rpm) reaction cell of 1.4 ml. Thirty-seven injections, each of 8-μl volume and 10-s duration with a 5-min interval between injections, were carried out using a 296-μl syringe filled with 1.0 mM ubiquitin solution. The calorimetric data were processed, and the binding affinity determined using the software ORIGIN (version 5.0) provided by the manufacturer.

Surface Plasmon Resonance (SPR)-based Biosensor Analysis — The interaction of UBA from EDD with the synthetic ubiquitin was analyzed by SPR (23) using a BIACORE 3000 optical biosensor (Biacore AB, Uppsala, Sweden). Protein dilutions were performed in running buffer, which contained 10 mM HEPES at pH 7.4, 150 mM NaCl, 3.4 mM EDTA, and 0.005% Tween 20. The concentration of EDD UBA was determined by hydrolysis and amino acid analysis. In a first series of experiments, monoubiquitin, K48-linked, K63-linked di- and tetraubiquitin were immobilized onto CM5 biosensor chip flow cells using amine coupling chemistry as described previously (23), leading to 2000 RUs of monoubiquitin, 3200 and 6300 RU of K63- and K48-diubiquitin, 11500 and 11000 RU of K48- and K63-tetraubiquitin. Biosensor experiments were repeated a minimum of two times and corrected for binding to a separate control flow cell (activated and blocked). The experiments were performed at 25 °C using a flow rate of 50 μl/min. For each experiment, at least 5 different concentrations of EDD UBA were injected over each experimental and control flow cell (1 min injections, extraclean procedure). In a second series of experiments, EDD UBA was biotinylated by addition and 90 min of incubation of 2 mg of EZ-Link® NHS-Chromogenic-Biotin (Pierce Biotechnology) to 0.6 μmol of EDD UBA in 1 ml buffer (10 mM HEPES pH 7.4, 150 mM NaCl) plus 200 μl Me_2SO. Biotinylated protein was purified by gel filtration and quantified by optical spectroscopy (354 nm). The biotinylated EDD UBA (85 RU) was captured onto a streptavidin-coated (SA) sensorchip flow cell previously prepared by three successive pulses of 1 M NaCl in 50 mM NaOH, according to the manufacturer's recommendations. Injections of monoubiquitin, K48- and N-to-C-linked diubiquitin were performed in duplicate over EDD UBA and control (streptavidin only) surfaces.

Thermodynamic dissociation constants (K_d) were determined using control-corrected plateau values; the K_d was

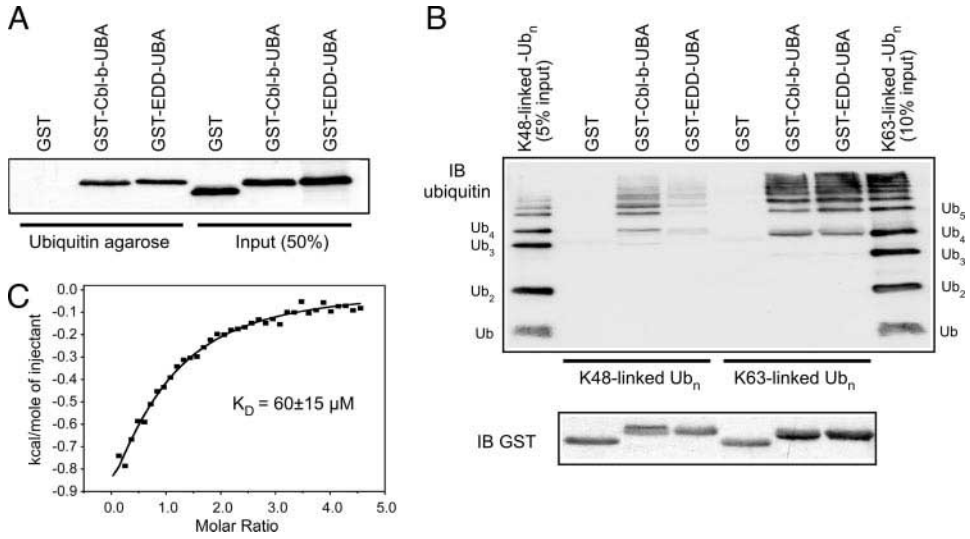

FIGURE 1. **The UBA domain of EDD binds to ubiquitin and polyubiquitin.** *A*, *in vitro* binding of the EDD and Cbl-b UBA domains to ubiquitin agarose. *B*, *in vitro* binding of the EDD and Cbl-b UBA domain to ubiquitin chains. *C*, calorimetric titration of the EDD UBA domain with ubiquitin. The panel shows the integrated heat released after correction for the heat of dilution (data points, *squares*) and the curve of best fit for binding to a single site.

derived from fitting of the experimental values. For analysis of ubiquitin chains binding to the UBA-derivatized surface, a global analysis was used in which the number of binding sites on the surface was constrained to be equal in all experiments.

Crystallization—Conditions were identified utilizing hanging drop vapor diffusion using the JCSG crystallization suite (Qiagen). The best crystals of the complex were obtained by equilibrating a 0.6-μl drop of an equimolar protein mixture (15 mg/ml total) in 20 mM Tris-HCl (pH 8.0), mixed with 0.6 μl of reservoir solution containing 0.1 M citric acid (pH 5.0) and 20% (w/v) PEG 6000 and suspended over 0.6 ml of reservoir solution. Crystals grew in 3–7 days at 20 °C. For data collection, crystals were picked up in a nylon loop and flash-cooled in a N_2 cold stream. The solution for cryoprotection contained the reservoir solution with addition of 20% (v/v) of glycerol. The crystals contained four UBA and four ubiquitin molecules in the asymmetric unit corresponding to $V_m = 2.2$ Å^3 Da^{-1} and a solvent content of 44% (24).

Structure Solution and Refinement—Diffraction data from a single crystal of the UBA-ubiquitin complex were collected on an ADSC Quantum-315 CCD detector (Area Detector Systems Corp.) at beamline X29 at the NSLS, Brookhaven National Laboratory (Table 1). Data processing and scaling were performed with HKL2000 (25). The structure was determined by molecular replacement with Phaser (26), using the coordinates of ubiquitin (PDB entry 1UBQ) and the UBA domain from Cbl-b (PDB entry 2OOA). The initial model obtained from Phaser was completed and adjusted with the program Xfit (27) and was improved by several cycles of refinement, using the program CNS v.1.1 (28) and model refitting. The refinement statistics are given in Table 1. Out of 53 residues in the UBA construct, the current model does not include residues Arg^{226}–Asp^{230} in chain B, Glu^{229}–Asp^{230} in chains D and F, and Asp^{228}–Asp^{230} in chain H. The three C-terminal residues of ubiquitin are also disordered in the chains A and G, while chains C and E are complete due to crystal packing. The final model has good stereochemistry (Table 1) according to the program PROCHECK (29). Figures were made with PyMOL.

NMR Spectroscopy—NMR resonance assignments of the ubiquitin-bound UBA domain from EDD ligase (3:1 ratio of ubiquitin to UBA) were carried out using ^{15}N-labeled and ^{13}C,^{15}N-labeled UBA samples. Protein signal assignments were performed using standard techniques, including three-dimensional experiments HNCACB, CBCA(CO)NH, and ^{15}N NOESY-HMQC. NMR samples contained 0.7–1.4 mM protein in 25 mM phosphate, 70 mM NaCl at pH 7.0. Signals for unliganded EDD UBA were reassigned using ^{15}N NOESY-HMQC. For NMR titrations, unlabeled ubiquitin was added to the ^{15}N-labeled 0.5–1.0 mM wild-type UBA or its mutants to the final molar ratio of 3 to 1 or 4 to 1, respectively. All NMR experiments were performed at 303 K using Varian 500 MHz and Bruker 600 MHz spectrometers. NMR spectra were processed using NMRPipe (30) and analyzed with XEASY (31).

RESULTS

EDD UBA Binds to Ubiquitin and Polyubiquitin Chains—To study the previously uncharacterized UBA domain, residues Ile^{180} to Asp^{230} of EDD were cloned for expression in *E. coli*. We tested its binding to ubiquitin using pull-down assays with ubiquitin agarose (Fig. 1*A*). EDD UBA bound to monoubiquitin with an affinity similar to that of the UBA domain from the Cbl-b ubiquitin ligase (21). Because many UBA domains have higher affinity for ubiquitin chains than for monoubiquitin, we also performed *in vitro* binding assays with K48- and K63-linked ubiquitin chains. While EDD UBA bound both forms of polyubiquitin, it displayed relatively higher affinity for K63-linked chains compared with the UBA domain from Cbl-b (Fig. 1*B*).

To further characterize the binding, we applied isothermal titration calorimetry (ITC) to determine binding constant and thermodynamic parameters of interactions between the EDD UBA domain and ubiquitin (Fig. 1*C*). The affinity (K_d) of the EDD UBA domain for monoubiquitin was measured to be 60 ± 15 μM, which is higher than the affinity of most characterized UBA domains (32) but again very similar to the affinity of Cbl-b (21).

EDD UBA Does Not Have Specificity for Ubiquitin Chains—We used surface plasmon resonance (SPR) experiments to verify the pull-down results and quantify the affinity of the EDD UBA domain for different ubiquitin chains (Fig. 2). Five different SPR surfaces were prepared and EDD UBA domain was injected over them (Fig. 2*A*). At the highest UBA concentration (0.55 mM), the binding curves did not reach saturation, which limited the extent of analysis possible. In addition, the surfaces

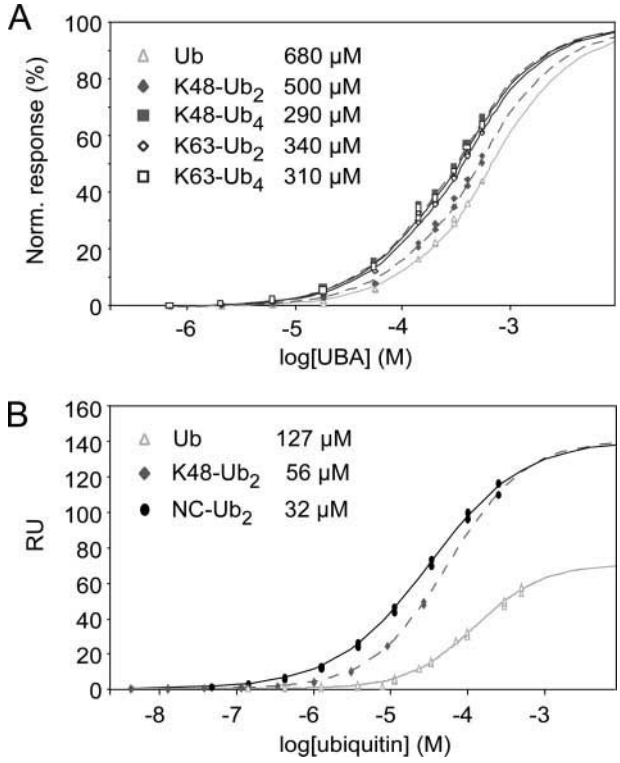

FIGURE 2. **Surface plasmon resonance of EDD UBA binding to ubiquitin and polyubiquitin chains.** *A*, EDD UBA injected over monoubiquitin (*Ub*, *open triangles*), K48-linked diubiquitin (*K48-Ub_2*, *dashed line* with *filled rhombus*), K48-linked tetraubiquitin (*K48-Ub_4*, *dashed line* with *filled squares*), K63-linked diubiquitin (*K63-Ub_2*, *open rhombus*), and K63-linked tetraubiquitin (*K63-Ub_4*, *open squares*) surfaces. Experimental data points and the fitted binding curves are shown. The data were fit without cooperativity between sites (a Hill coefficient of 1) and normalized by the maximum response for each surface. Maximum responses were 770 (Ub), 1190 (K48-Ub_2), 3340 (K48-Ub_4), 2270 (K63-Ub_2), and 3870 (K63-Ub_4) in response units (*RU*). *B*, ubiquitin and polyubiquitin flowing over a UBA surface. Data and fitted curves are shown for monoubiquitin (*Ub*, *open triangles*), K48-linked diubiquitin (*K48-Ub_2*, *dashed line with filled rhombus*), and N-to-C-linked diubiquitin (*NC-Ub_2*, *filled oval*). The data were fit to allow cooperativity between sites with Hill coefficients of 0.99 (Ub), 0.87 (K48-Ub_2), and 0.71 (NC-Ub_2).

TABLE 1
Data collection and refinement statistics

	EDD UBA/ubiquitin
Data collection	
Space group	$P2_12_12_1$
Cell dimensions	
a, *b*, *c* (Å)	33.85, 59.33, 246.67
Resolution (Å)	50-1.85 (1.92-1.85)[a]
R_{merge}	0.051 (0.292)
I/σI	29.5 (7.1)
Completeness (%)	93.3 (81.0)
Redundancy	7.0 (5.7)
Refinement	
Resolution (Å)	50-1.85
No. reflections	38635
R_{work}/R_{free}	0.207/0.258
No. atoms	4145
Protein	3841
Water	304
B-factors	
Protein	15.61
Water	20.65
R.m.s deviations	
Bond lengths (Å)	0.018
Bond angles (°)	1.72
Ramachandran statistics (%)	
Residues in favored regions	94.2
Residues in additionally allowed regions	5.8

[a] Highest resolution shell is shown in parentheses.

appeared to suffer from heterogeneity resulting from multiple modes of ubiquitin and polyubiquitin coupling to the surface. This led to large overestimates of the K_d's but still allowed qualitative comparisons between surfaces. As a control, the UBA domain of Mud1 was used (33).

K_d values of EDD UBA for the polyubiquitin surfaces were roughly half the K_d for monoubiquitin (Fig. 2*A*). The UBA domain showed slightly better affinity for K63-diubiquitin than for K48-diubiquitin but there was no difference between the two tetraubiquitin surfaces. In contrast, the Mud1 UBA showed a 5-fold preference for K48-linked polyubiquitin with K_d values of 58 μM for the K48-Ub_4 surface and 283 μM for the K63-Ub_4 surface (supplemental Fig. S1). Our conclusion is that unlike Mud1, the UBA domain from EDD did not show markedly higher affinity for the K48- or K63-linked polyubiquitin surfaces.

We also carried out reciprocal SPR experiments injecting ubiquitin chains over a surface on which the EDD UBA domain had been captured (Fig. 2*B*). Although we were limited by the amounts and types of ubiquitin chains that could be used, this second approach had the advantage that a single surface could be used to compare affinities. The lower loading of the surface also significantly improved the agreement between affinity of monoubiquitin measured by SPR (127 μM) and ITC (60 μM). On the UBA surface, K48-linked and N-to-C diubiquitin both bound with higher affinity than monoubiquitin but also with detectable negative cooperativity (Fig. 2*B*). The K_d for N-to-C diubiquitin was half that of K48-diubiquitin, consistent with the more open conformation of this type of chain in solution (34).

The results from the SPR experiments suggest that the EDD UBA domain binds to polyubiquitin relatively poorly compared with other UBA domains (20, 33). The higher apparent affinity for polyubiquitin results from the larger number monoubiquitin units available for binding (avidity effects) and is not due to specific recognition of polyubiquitin chains. K63-linked and N-to-C chains showed better binding due to the more open conformation of these types of chains (34). In contrast, K48-linked chains bound somewhat less well due to their relatively closed conformation where competition exists between ubiquitin-ubiquitin interactions and UBA binding (35).

Structure of EDD UBA—To understand the structural basis of the ubiquitin-binding properties of EDD UBA, we co-crystallized ubiquitin with the EDD UBA domain and solved the structure of the complex at 1.85-Å resolution (Table 1). The crystals contained four UBA-ubiquitin complexes in the asymmetric unit. All four complexes were nearly identical; their backbone atoms could be overlaid with an r.m.s.d. of 0.37 Å. The UBA structures themselves could be overlaid with an r.m.s.d. of 0.29 Å.

The EDD fragment shows the canonical UBA fold consisting of a three-helical bundle (α1–α3) (Fig. 3). The domain has a well-defined hydrophobic core that includes Ile^{190}, Ala^{193}, Leu^{197}, Ile^{205}, Leu^{209}, Ala^{219}, and Leu^{223} (Fig. 3*A*). Among the

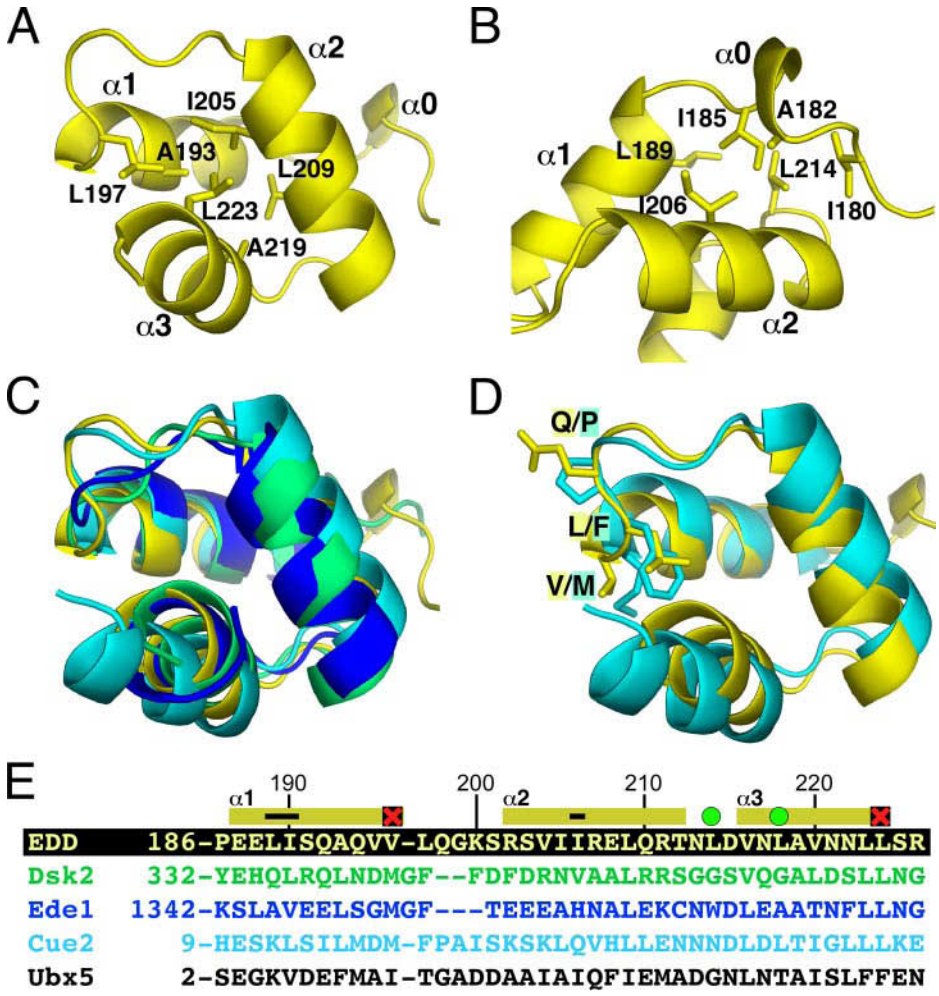

FIGURE 3. **Structure of the EDD fragment containing the UBA domain and its comparison with other UBA/CUE domains.** *A*, *ribbon representation* of the EDD UBA domain. The residues forming hydrophobic core are shown as *sticks* and labeled. Helices are labeled from α0 to α3. *B*, hydrophobic residues of the α1–α2 surface contact hydrophobic residues in the α0 helix. *C*, backbone overlay of the EDD UBA structure (*yellow*) with Dsk2 (*green*), Ede1 (*dark blue*), and Cue2 (*light blue*) structures. *D*, residues in the α1–α2 loop of EDD and Cue2. The loop conformation is strikingly similar in the UBA and CUE domain structures despite the different amino acids sequence. *E*, sequence alignment of the UBA domains from EDD, Dsk2, Ede1, and Ubx5 and CUE domain from Cue2. The α-helices and locations of amino acid substitutions in EDD that destabilize the protein (*horizontal bars*), that block ubiquitin binding (*red X*), or that have no effect (*green circles*) are shown.

notable features, the N-terminal portion before the UBA domain contains a short helical turn that packs against helices α1 and α2. This α0-helix covers the hydrophobic patch consisting of Ile[190], Ile[206], and Leu[214] that would be otherwise solvent-exposed (Fig. 3*B*). Residues Ile[180]–Pro[186] adopted an essentially identical conformation in all four copies in asymmetric unit, which suggests that the α0-helix is structurally relevant. In addition, mutagenesis of Leu[189], Ile[190], and Ile[206] destabilized the protein (see below). On the other hand, NMR experiments showed that the helix is only partially populated. Heteronuclear NOEs revealed that the Ile[180]–Ser[183] region is relatively mobile in solution (supplemental Fig. S2) and ^{15}N NOESY NMR data did not show the medium range NOEs characteristic of a helical turn (data not shown).

Superposition of the EDD UBA structure with related structures reveals that EDD UBA is structurally similar to CUE (coupling of ubiquitin conjugation to endoplasmic reticulum degradation) domains. CUE domains are a conserved monoubiquitin-binding fold that resembles UBA domains at the level of amino acid sequence, size, tertiary fold, and ubiquitin binding (18, 36) but are distinguished by a longer α1–α2 loop containing an MFP signature motif. The EDD UBA α1–α2 loop adopts a conformation identical to that of CUE domain structures with residues Val[196]-Leu[197]-Gln[198] superimposable on the MFP motif (Fig. 3*D*). Leu[197] from the α1–α2 loop is part of the hydrophobic core and stacks against Leu[223]. The loop is relatively rigid in solution as evidenced by heteronuclear NOEs (supplemental Fig. S2).

EDD UBA-Ubiquitin Recognition Elements—The UBA/ubiquitin intermolecular interface consists of the β-sheet surface of ubiquitin and helix α3 and the C terminus of helix α1 of EDD UBA (Fig. 4*A*). The majority of interactions are hydrophobic. The side chain of Val[196] fits into a hydrophobic pocket formed by the side chains of Leu[8], His[68], and Val[70] of ubiquitin (Fig. 4*B*). Half a turn earlier, the aliphatic atoms of Gln[192] interact with the side chain of Leu[8]. The side chain of Gln[198] in the α1–α2 loop contacts the backbone of Ala[46]. The full length of helix α3 is involved in ubiquitin binding starting with the side chain of Val[216] that contacts ubiquitin Leu[8]. Leu[224] is another crucial determinant of ubiquitin recognition as its side chain binds in a groove formed by Val[70], Ile[44], Gln[49], and Arg[42] of ubiquitin (Fig. 4*C*).

The hydrophobic interactions between the EDD UBA domain and ubiquitin are strengthened by a variety of hydrogen bonds. The side chain of Asn[221] makes hydrogen bonds with the backbone carbonyl of Leu[71] and the side chain of Arg[42], which also hydrogen bonds with the side chain of Ser[225] (Fig. 4*D*). The carbonyl of Leu[224] forms a hydrogen bond with the side chain of Gln[49]. The structure also reveals intermolecular hydrogen bonds involving ordered water molecules. Thus, carbonyl of Val[196] hydrogen bonds with amide of Gly[47] via a bound water molecule (Fig. 4*E*). Similarly, another water molecule bridges the side chain of Asn[217] and the amide of Leu[71] (Fig. 4*F*). Notably, the above-mentioned ionic interactions were observed in all four copies of the EDD UBA/ubiquitin structure and, thus, unlikely to be affected by crystal packing.

NMR Confirms the Ubiquitin-binding Site in EDD UBA—To verify the mechanism of ubiquitin recognition in solution, EDD UBA was expressed in media supplemented with $^{15}NH_4Cl$. The

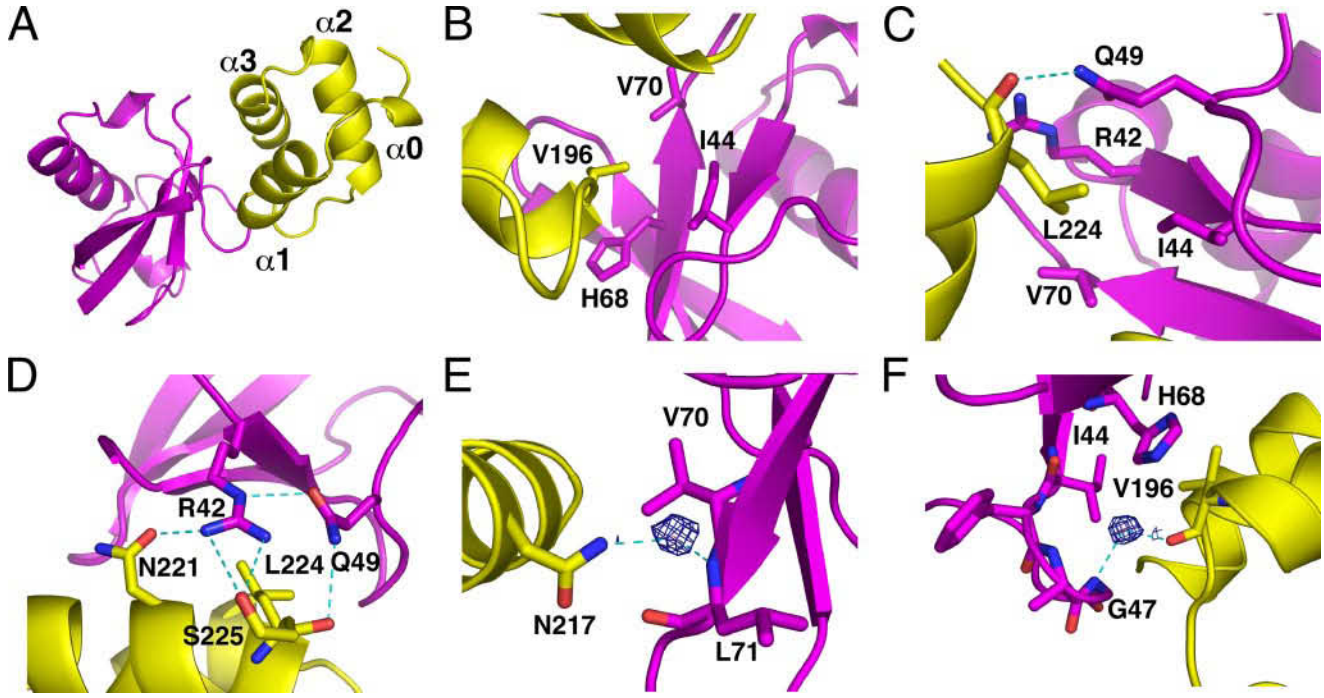

FIGURE 4. **Crystal structure of the EDD UBA-ubiquitin complex.** *A*, overall structure of the complex. Ubiquitin is in *yellow*, and the UBA domain is in *purple*. *B*, UBA Val^{196} binds the hydrophobic groove formed by Ile^{44}, His^{68}, and Val^{70} of ubiquitin. *C*, UBA Leu^{224} binds the groove formed by Ile^{44}, Arg^{42}, Gln^{49}, and Val^{70} of ubiquitin. *D*, Arg^{42} and Gln^{49} of ubiquitin form a network of intermolecular hydrogen bonds with Asn^{221} and Ser^{225} of EDD UBA. *E*, amide of Gly^{47} of ubiquitin forms an intermolecular hydrogen bond with carbonyl of Val^{216} of EDD UBA via a bound water molecule. *F*, bound water molecule facilitates hydrogen bonding between amide of Leu^{71} of ubiquitin and side chain of Asn^{217} of EDD UBA. The $2F_o$-F_c electron density (1σ contour, omit map) for bound water molecules is shown in *panels E* and *F*.

^{15}N-^{1}H correlation spectra of the unliganded domain showed the good dispersion of signals characteristic of a folded protein but with heterogeneity in peak heights suggesting the existence of conformational exchange or aggregation (supplemental Fig. S3). Addition of unlabeled ubiquitin caused chemical shift changes for a limited number of UBA residues and, notably, sharpened the broad signals in the NMR spectra, making them amenable to assignment using standard heteronuclear experiments with double-labeled protein. As a result, all signals of the ubiquitin-bound form were assigned with the exception of missing signals from the N-terminal Gly-Ser cloning linker (Fig. 5*A*). These assignments and NMR titration spectra were used to assign the signals in ligand-free EDD UBA, which were then verified using an ^{15}N NOESY experiment.

The residues displaying the largest chemical shift changes upon ubiquitin binding were Gln^{198} (0.57), Ala^{193} (0.46), Val^{196} (0.44), Leu^{197} (0.42), and Asn^{217} (0.32) (Fig. 5*B*). The changes are grouped at the C-terminal part of helix α1, the α1–α2 loop, and helix α3 (Fig. 5*C*). This is similar to most UBA and CUE domains (19, 33, 37–42). The large chemical shift changes in the α1–α2 loop was somewhat unexpected, since EDD does not possess the conserved methionine residue usually found in this loop as part of the MGF motif required for ubiquitin recognition.

Site-directed Mutagenesis—We prepared seven point mutants of EDD UBA and tested their binding to ubiquitin in *in vitro* pull-down assays (Fig. 6). Mutants V196K, L214N, L218K, and L224K were confirmed to be correctly folded as verified using two-dimensional HSQC NMR spectra; the three remaining mutants L189K, I190K, and I206K were partially unfolded (data not shown and supplemental Fig. S3). The destabilized mutations are located at the interface with helix α0 (Fig. 3*B*), which is consistent with the importance of this helix in stabilizing the structure of the isolated EDD UBA domain.

Among the folded mutants, the V196K and L224K substitutions completely abrogated binding to ubiquitin-agarose (Fig. 6*B*) and pull-down of K48- and K63-linked polyubiquitin (Fig. 6, *C* and *D*). The lack of ubiquitin binding was confirmed by NMR experiments: a 4-fold excess of ubiquitin did not produce observable chemical shift changes in the HSQC spectra (data not shown). The mutants I206K (which could fold in the presence of ubiquitin), L214N, and L218K showed binding to both monoubiquitin and polyubiquitin chains (Fig. 6). Significantly, we found no evidence of mutations that would differentially affect K48- or K63-linked polyubiquitin binding.

DISCUSSION

This work reports the structure of a previously uncharacterized UBA domain from EDD. We show that the domain binds to ubiquitin and present a comprehensive molecular characterization of the EDD UBA/ubiquitin interactions. EDD was first classified as a ubiquitin ligase based on the presence of catalytic HECT domain. Ubiquitin binding by the UBA domain provides another link for the involvement of EDD in the ubiquitin-mediated processes.

Previous UBA-ubiquitin complex structures exhibit two distinct binding modes. While most UBA domains recognize ubiquitin and ubiquitin-like domains via the α1–α2 loop and helix α3 (18, 19, 37, 39, 41–43), the UBA domain from Cbl-b ubiquitin ligase binds to ubiquitin using helix α1 (21). The EDD

UBA-ubiquitin structure is largely similar to the former group which also includes CUE-ubiquitin complexes (38, 44). The distinction between UBA and CUE domains is blurred by the EDD UBA domain, which contains elements of both families.

The structure also underlines the challenges of sequence alignment of UBA domains, which results from their small size and low sequence identity. The initial motivation for structural studies of EDD UBA was to explain ubiquitin binding by EDD, which lacks the conserved methionine residue found in the $\alpha1-\alpha2$ loop of other UBA domains. The structure revealed that the EDD possesses two extra residues in the $\alpha1-\alpha2$ loop, which positions a hydrophobic residue, valine, in place of the conserved methionine. The larger $\alpha1-\alpha2$ loop is a characteristic of CUE domains but may occur in other UBA domains, such as the domain from the Ubx5 protein (also called YDR330w) (45). The Ubx5 UBA domain aligns well with EDD UBA and contains isoleucine at the position corresponding to Val[196] of EDD UBA (Fig. 3*E*).

The EDD UBA-ubiquitin structure explains how a smaller hydrophobic residue, valine, can replace the larger methionine residue. Superposition of five complexes shows that the EDD UBA is slightly shifted relative to ubiquitin compared with other UBA/CUE domains (Fig. 7). In helix $\alpha1$, this moves the side chain of Val[196] so that it occupies the same position as the methionine residue in other complexes with ubiquitin. The shift also leads to a larger distance between carbonyl of Val[196] and amide of Gly[47] of ubiquitin, which are unable to form the direct hydrogen bond seen in other UBA-ubiquitin complexes. Interestingly, this intermolecular interaction is preserved in the EDD UBA/ubiquitin

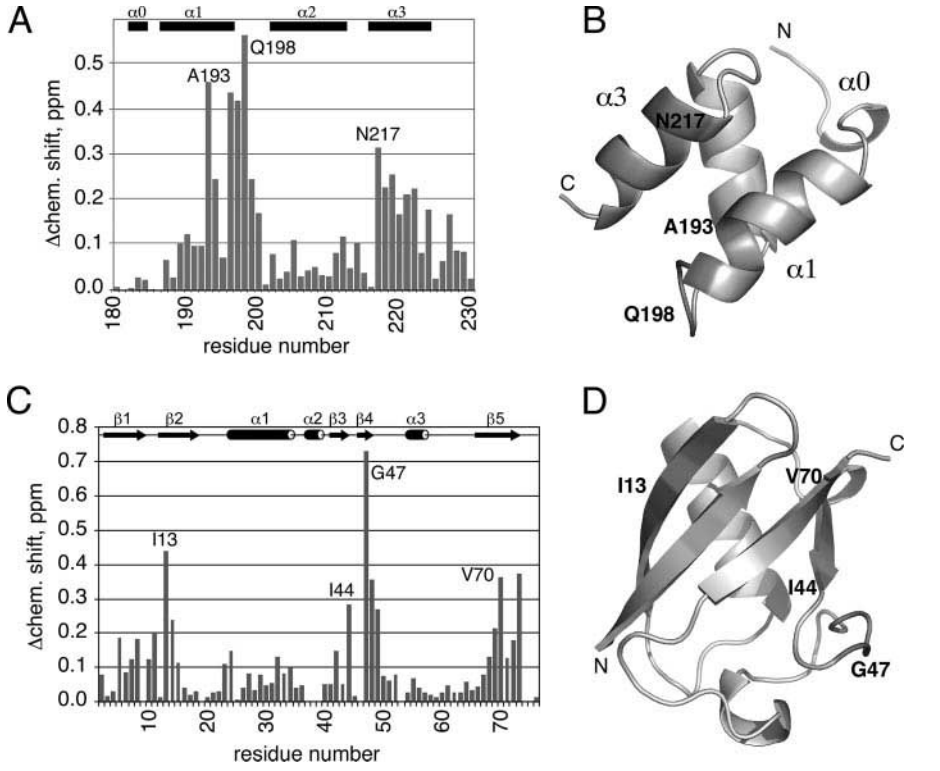

FIGURE 5. **NMR mapping of EDD UBA-ubiquitin interactions in solution.** *A*, ^{1}H-^{15}N HSQC spectrum of the EDD UBA domain bound to ubiquitin. Signals are labeled with the *one-letter amino acid code* and residue number. Signals from asparagine and glutamine side chains are marked with *horizontal lines*. For clarity, peaks in the center of the spectrum are not labeled. *B*, plot of amide chemical shift changes of the UBA domain from EDD upon binding to monoubiquitin. The chemical shift changes were calculated as $(\Delta HN^2 + (0.2 \times \Delta N)^2)^{1/2}$. The most affected residues are labeled. Secondary structure elements are shown *above* the plot. Plot (*C*), and mapping (*D*) of the chemical shift changes in EDD UBA upon ubiquitin binding. *Gray* indicates a large chemical shift change; *white* indicates no change.

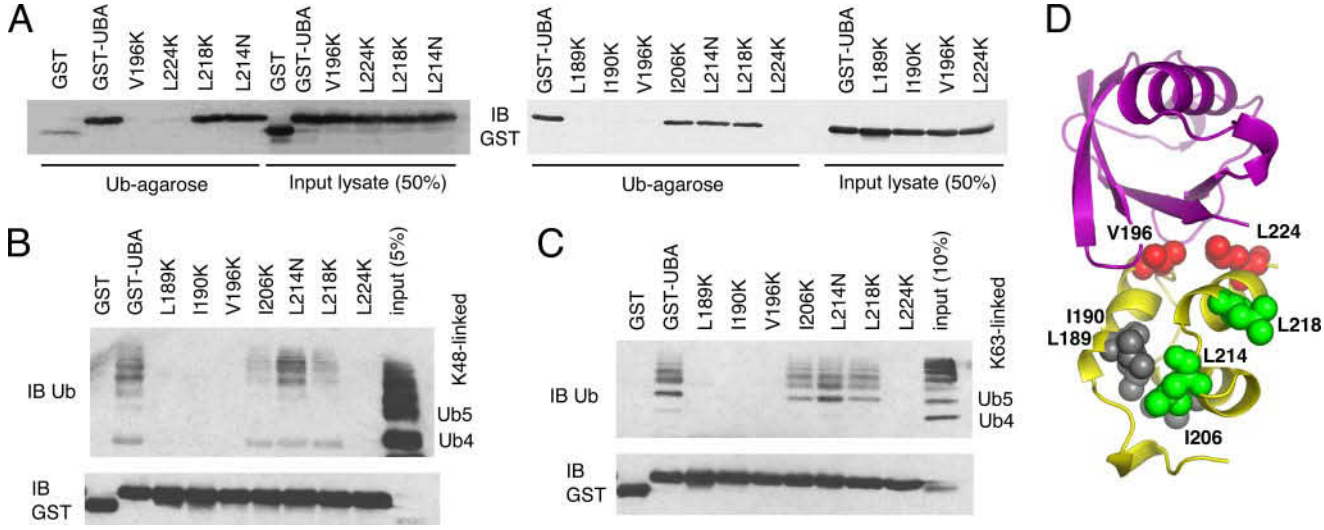

FIGURE 6. **Val[196] and Leu[224] of the UBA domain of EDD are required for ubiquitin binding.** *A*, binding of mutant EDD UBA GST-fusion proteins to ubiquitin agarose. *B*, binding of K48-linked ubiquitin chains to immobilized GST-UBA mutants. *C*, binding of K63-linked ubiquitin chains to immobilized GST-UBA mutants. *D*, mutated UBA residues in the x-ray structure of the UBA-ubiquitin complex. Residues required for binding are colored *red* (V196K, L224K), permissive residues are *green* (L214N, L218K), and residues that destabilized the UBA domain when mutated are colored *gray* (L189K, I190K, L206K).

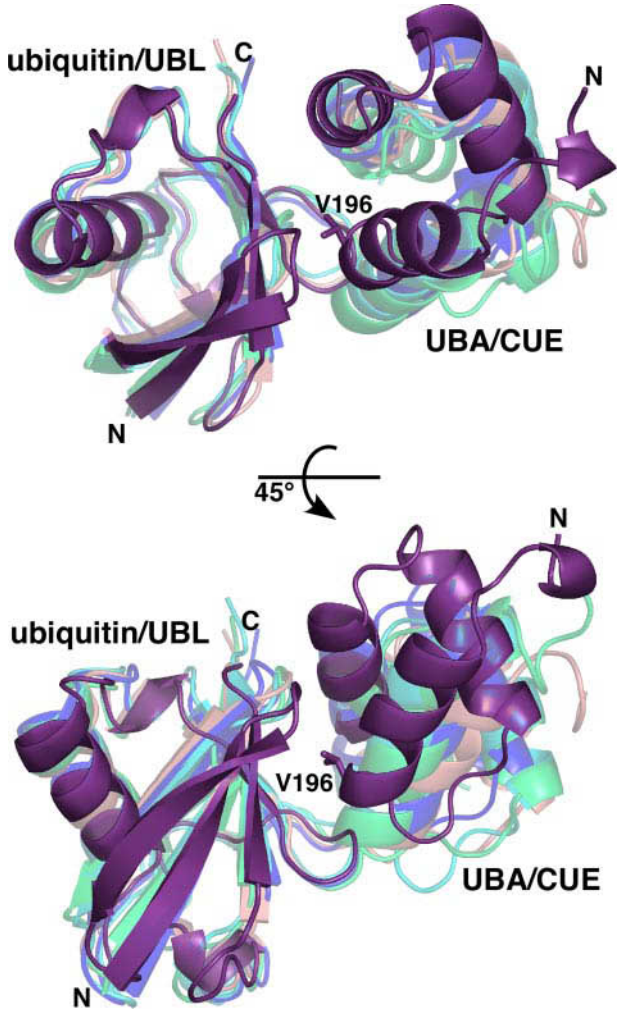

FIGURE 7. **Overlay of five complexes of ubiquitin/UBL and UBA/CUE domains.** The UBA domain of EDD binds to ubiquitin in a fashion similar to other UBA and CUE domains. The structures are ubiquitin and UBA domain of EDD (*purple*, this work), the ubiquitin and the UBA domain of Dsk2 (*green*, PDB accession code 1WR1), the ubiquitin, and the UBA domain of Ede1 (*dark-blue*, PDB 2G3Q), ubiquitin and the CUE domain of Cue2 (*teal*, PDB 1OTR), and a UBL domain complexed with the UBA domain of Dsk2 (*coral*, PDB 2BWE). The side chain of Val^{196} of EDD UBA is shown.

structure via a bound water molecule. The EDD UBA-ubiquitin structure reveals novel intermolecular ionic interactions, most of them involving Arg^{42} of ubiquitin that forms a network of intra- and intermolecular hydrogen bonds (Fig. 4*D*). Perhaps, due to more extensive polar intermolecular interactions, the buried surface (725 $Å^2$) of the EDD UBA/ubiquitin complex is larger than that of ubiquitin bound to the UBA domains of Ede1 (19) (370 $Å^2$) and Dsk2p (18) (480 $Å^2$).

Our results show that the EDD UBA domain does not bind polyubiquitin chains significantly more tightly than monoubiquitin. Monoubiquitination is a common post-translational modification in DNA damage repair pathways. Monoubiquitinated proliferating cell nuclear antigen (PCNA) activates translesion DNA synthesis by damage-tolerant polymerases in yeast leading to DNA damage-induced mutagenesis (46). In another example, FANCD2, a protein involved in Fanconi Anemia, is monoubiquitinated upon DNA damage and recruited to chromatin-associated nuclear foci, where it interacts with BRCA1 and other DNA repair enzymes (47). Interestingly, EDD is also involved in DNA damage signaling via ubiquitinylation of TopB1 (7), which co-localizes with BRCA1 at stalled replication forks (7, 8). Understanding of ubiquitin binding properties of EDD ubiquitin ligase provides a basis for functional studies of its importance for the EDD family of proteins.

Acknowledgments—We thank Simon Wing (McGill University) for the gift of EDD cDNA. We thank Tara Sprules for help in running NMR experiments at the Quebec-Eastern Canada High-Field NMR Facility and Jean-François Trempe for valuable discussions and the gift of purified Mud1 UBA. We thank Allan Matte and Annie Héroux for data collection. Data for this study were measured at beamline X29 of the National Synchrotron Light Source, supported by the Offices of Biological and Environmental Research and of Basic Energy Sciences of the United States Department of Energy and the National Center for Research Resources of the National Institutes of Health.

REFERENCES

1. Kwon, Y. T., Reiss, Y., Fried, V. A., Hershko, A., Yoon, J. K., Gonda, D. K., Sangan, P., Copeland, N. G., Jenkins, N. A., and Varshavsky, A. (1998) *Proc. Natl. Acad. Sci. U. S. A.* **95,** 7898–7903
2. Huibregtse, J. M., Scheffner, M., Beaudenon, S., and Howley, P. M. (1995) *Proc. Natl. Acad. Sci. U. S. A.* **92,** 2563–2567
3. Mansfield, E., Hersperger, E., Biggs, J., and Shearn, A. (1994) *Dev. Biol.* **165,** 507–526
4. Callaghan, M. J., Russell, A. J., Woollatt, E., Sutherland, G. R., Sutherland, R. L., and Watts, C. K. (1998) *Oncogene* **17,** 3479–3491
5. Clancy, J. L., Henderson, M. J., Russell, A. J., Anderson, D. W., Bova, R. J., Campbell, I. G., Choong, D. Y., Macdonald, G. A., Mann, G. J., Nolan, T., Brady, G., Olopade, O. I., Woollatt, E., Davies, M. J., Segara, D., Hacker, N. F., Henshall, S. M., Sutherland, R. L., and Watts, C. K. (2003) *Oncogene* **22,** 5070–5081
6. Fuja, T. J., Lin, F., Osann, K. E., and Bryant, P. J. (2004) *Cancer Res.* **64,** 942–951
7. Honda, Y., Tojo, M., Matsuzaki, K., Anan, T., Matsumoto, M., Ando, M., Saya, H., and Nakao, M. (2002) *J. Biol. Chem.* **277,** 3599–3605
8. Makiniemi, M., Hillukkala, T., Tuusa, J., Reini, K., Vaara, M., Huang, D., Pospiech, H., Majuri, I., Westerling, T., Makela, T. P., and Syvaoja, J. E. (2001) *J. Biol. Chem.* **276,** 30399–30406
9. Henderson, M. J., Munoz, M. A., Saunders, D. N., Clancy, J. L., Russell, A. J., Williams, B., Pappin, D., Khanna, K. K., Jackson, S. P., Sutherland, R. L., and Watts, C. K. (2006) *J. Biol. Chem.* **281,** 39990–40000
10. Henderson, M. J., Russell, A. J., Hird, S., Munoz, M., Clancy, J. L., Lehrbach, G. M., Calanni, S. T., Jans, D. A., Sutherland, R. L., and Watts, C. K. (2002) *J. Biol. Chem.* **277,** 26468–26478
11. Eblen, S. T., Kumar, N. V., Shah, K., Henderson, M. J., Watts, C. K., Shokat, K. M., and Weber, M. J. (2003) *J. Biol. Chem.* **278,** 14926–14935
12. Yoshida, M., Yoshida, K., Kozlov, G., Lim, N. S., De Crescenzo, G., Pang, Z., Berlanga, J. J., Kahvejian, A., Gehring, K., Wing, S. S., and Sonenberg, N. (2006) *EMBO J.* **25,** 1934–1944
13. Tasaki, T., Mulder, L. C., Iwamatsu, A., Lee, M. J., Davydov, I. V., Varshavsky, A., Muesing, M., and Kwon, Y. T. (2005) *Mol. Cell Biol.* **25,** 7120–7136
14. Hofmann, K., and Bucher, P. (1996) *Trends Biochem. Sci.* **21,** 172–173
15. Hurley, J. H., Lee, S., and Prag, G. (2006) *Biochem. J.* **399,** 361–372
16. Dieckmann, T., Withers-Ward, E. S., Jarosinski, M. A., Liu, C. F., Chen, I. S., and Feigon, J. (1998) *Nat. Struct. Biol.* **5,** 1042–1047
17. Mueller, T. D., and Feigon, J. (2002) *J. Mol. Biol.* **319,** 1243–1255
18. Ohno, A., Jee, J., Fujiwara, K., Tenno, T., Goda, N., Tochio, H., Kobayashi, H., Hiroaki, H., and Shirakawa, M. (2005) *Structure.* **13,** 521–532
19. Swanson, K. A., Hicke, L., and Radhakrishnan, I. (2006) *J. Mol. Biol.* **358,** 713–724
20. Raasi, S., Varadan, R., Fushman, D., and Pickart, C. M. (2005) *Nat. Struct.*

Mol. Biol. **12,** 708–714
21. Peschard, P., Kozlov, G., Lin, T., Mirza, I. A., Berghuis, A. M., Lipkowitz, S., Park, M., and Gehring, K. (2007) *Mol. Cell* **27,** 474–485
22. Kozlov, G., Peschard, P., Zimmerman, B., Lin, T., Moldoveanu, T., Mansur-Azzam, N., Gehring, K., and Park, M. (2007) *J. Biol. Chem.* **282,** 27547–27555
23. Jonsson, U., Fagerstam, L., Ivarsson, B., Johnsson, B., Karlsson, R., Lundh, K., Lofas, S., Persson, B., Roos, H., Ronnberg, I., Sjulander, S., Stenberg, E., Stahlberg, R., Urbaniczky, C., Ostlin, H., and Malmqvist, M. (1991) *BioTechniques* **11,** 620–627
24. Matthews, B. W. (1968) *J. Mol. Biol.* **33,** 491–497
25. Otwinowski, Z., and Minor, W. (1997) *Methods Enzymol.* **276,** 307–326
26. Read, R. J. (2001) *Acta Crystallogr. D Biol. Crystallogr.* **57,** 1373–1382
27. McRee, D. E. (1999) *J. Struct. Biol.* **125,** 156–165
28. Brunger, A. T., Adams, P. D., Clore, G. M., DeLano, W. L., Gros, P., Grosse-Kunstleve, R. W., Jiang, J. S., Kuszewski, J., Nilges, M., Pannu, N. S., Read, R. J., Rice, L. M., Simonson, T., and Warren, G. L. (1998) *Acta Crystallogr. D Biol. Crystallogr.* **54,** 905–921
29. Laskowski, R. A., MacArthur, M. W., Moss, D. S., and Thornton, J. M. (1993) *J. Appl. Crystallogr.* **26,** 283–291
30. Delaglio, F., Grzesiek, S., Vuister, G. W., Zhu, G., Pfeifer, J., and Bax, A. (1995) *J. Biomol. NMR* **6,** 277–293
31. Bartels, C., Xia, T. H., Billeter, M., Guntert, P., and Wuthrich, K. (1995) *J. Biomol. NMR* **6,** 1–10
32. Hicke, L., Schubert, H. L., and Hill, C. P. (2005) *Nat. Rev. Mol. Cell Biol.* **6,** 610–621
33. Trempe, J. F., Brown, N. R., Lowe, E. D., Gordon, C., Campbell, I. D., Noble, M. E., and Endicott, J. A. (2005) *EMBO J.* **24,** 3178–3189
34. Varadan, R., Assfalg, M., Haririnia, A., Raasi, S., Pickart, C., and Fushman, D. (2004) *J. Biol. Chem.* **279,** 7055–7063
35. Varadan, R., Walker, O., Pickart, C., and Fushman, D. (2002) *J. Mol. Biol.* **324,** 637–647
36. Shih, S. C., Prag, G., Francis, S. A., Sutanto, M. A., Hurley, J. H., and Hicke, L. (2003) *EMBO J.* **22,** 1273–1281
37. Chang, Y. G., Song, A. X., Gao, Y. G., Shi, Y. H., Lin, X. J., Cao, X. T., Lin, D. H., and Hu, H. Y. (2006) *Protein Sci.* **15,** 1248–1259
38. Kang, R. S., Daniels, C. M., Francis, S. A., Shih, S. C., Salerno, W. J., Hicke, L., and Radhakrishnan, I. (2003) *Cell* **113,** 621–630
39. Ryu, K. S., Lee, K. J., Bae, S. H., Kim, B. K., Kim, K. A., and Choi, B. S. (2003) *J. Biol. Chem.* **278,** 36621–36627
40. Varadan, R., Assfalg, M., Raasi, S., Pickart, C., and Fushman, D. (2005) *Mol. Cell* **18,** 687–698
41. Wang, Q., Goh, A. M., Howley, P. M., and Walters, K. J. (2003) *Biochemistry* **42,** 13529–13535
42. Mueller, T. D., Kamionka, M., and Feigon, J. (2004) *J. Biol. Chem.* **279,** 11926–11936
43. Lowe, E. D., Hasan, N., Trempe, J. F., Fonso, L., Noble, M. E., Endicott, J. A., Johnson, L. N., and Brown, N. R. (2006) *Acta Crystallogr. D Biol. Crystallogr.* **62,** 177–188
44. Prag, G., Misra, S., Jones, E. A., Ghirlando, R., Davies, B. A., Horazdovsky, B. F., and Hurley, J. H. (2003) *Cell* **113,** 609–620
45. Schuberth, C., Richly, H., Rumpf, S., and Buchberger, A. (2004) *EMBO Rep.* **5,** 818–824
46. Stelter, P., and Ulrich, H. D. (2003) *Nature* **425,** 188–191
47. Garcia-Higuera, I., Taniguchi, T., Ganesan, S., Meyn, M. S., Timmers, C., Hejna, J., Grompe, M., and D'Andrea, A. D. (2001) *Mol. Cell* **7,** 249–262